

# Future research program on prompt $\gamma$ -ray emission in nuclear fission<sup>\*</sup>

S. Oberstedt<sup>1,a</sup>, R. Billnert<sup>1,2</sup>, F.-J. Hamsch<sup>1</sup>, M. Lebois<sup>3</sup>, A. Oberstedt<sup>2,4</sup>, and J.N. Wilson<sup>3</sup>

<sup>1</sup> European Commission, Joint Research Centre IRMM, 2440 Geel, Belgium

<sup>2</sup> Fundamental Fysik, Chalmers Tekniska Högskola, 41296 Göteborg, Sweden

<sup>3</sup> Institut de Physique Nucleaire Orsay, 91406 Orsay, France

<sup>4</sup> Ossolution Consulting, 70353 Örebro, Sweden

Received: 5 May 2015 / Revised: 9 July 2015

Published online: 23 December 2015

© The Author(s) 2015. This article is published with open access at Springerlink.com

Communicated by N. Alamanos

**Abstract.** In recent years the measurement of prompt fission  $\gamma$ -ray spectra (PFGS) has gained renewed interest, after about forty years since the first comprehensive studies of the reactions  $^{235}\text{U}(n_{th}, f)$ ,  $^{239}\text{Pu}(n_{th}, f)$  and  $^{252}\text{Cf}(sf)$ . The renaissance was initiated by requests for new values especially for  $\gamma$ -ray multiplicity and average total energy release per fission in neutron-induced fission of  $^{235}\text{U}$  and  $^{239}\text{Pu}$ . Both isotopes are considered the most important ones with respect to the modeling of innovative cores required for the Generation-IV reactors, the majority working with fast neutrons. During the last 5 years we have conducted a systematic study of spectral data for thermal-neutron-induced fission on  $^{235}\text{U}$  and  $^{241}\text{Pu}$  as well as for the spontaneous fission of  $^{252}\text{Cf}$  with unprecedented accuracy. From the new data we conclude that those reactions do not considerably contribute to the observed heat excess and suspect other reactions playing a significant role. Possible contributions may originate from fast-neutron-induced reactions on  $^{238}\text{U}$ , which is largely present in the fuel, or from  $\gamma$ -induced fission from neutron capture in the construction material. A first experiment campaign on prompt  $\gamma$ -ray emission from fast-neutron-induced fission on  $^{235,238}\text{U}$  was successfully performed in order to test our assumptions. In the following we attempt to summarize, what has been done in the field to date, and to motivate future measurement campaigns exploiting dedicated neutron and photon beams as well as upcoming highly efficient detector assemblies.

## 1 Introduction

The energy released in nuclear fission is distributed in kinetic and excitation energy of the two fragments. The excitation energy manifests itself in fragment deformation and intrinsic excitation energy, which subsequently is released by the emission of prompt neutrons and  $\gamma$ -rays and, at a later stage, through  $\beta$ -decay towards isotopes in the valley of stability. The first step of de-excitation contributes to the prompt heat released in fission, whereas the second, delayed step is counted as decay heat. Properties of the emitted particles prior to the onset of weak decays are important for nuclear applications as well as for the better understanding of the mechanism of fission-fragment de-excitation. Whilst prompt fission neutron emission is being studied during the last 50 years, see, *e.g.*, refs. [1–6], prompt  $\gamma$ -ray emission was investigated essentially in the

early 1970 years and only for a limited number of fissioning isotopes. From measured prompt fission  $\gamma$ -ray spectra (PFGS) average values for the total energy release per fission and  $\gamma$ -multiplicity were obtained.

The principal difficulty in prompt fission  $\gamma$ -ray measurements is the wide-spread time distribution, which covers the region from below picoseconds up to several microseconds. The obtained spectral data are, therefore, very sensitive to the particular experiment set-up, the covered time region as well as to the energy range of the emitted  $\gamma$ -rays. An inherent problem of such measurements is the sufficient discrimination of prompt fission neutrons, which may induce the production of  $\gamma$ -rays through inelastic scattering in the detector and the surrounding materials, finally mixing with the signal from prompt fission  $\gamma$ -rays.

In the end, those data entered in evaluated nuclear data libraries [7, 8] at both thermal and 14.6 MeV neutron energies, neglecting a possible dependence on the incoming neutron energy. In addition, those few spectra were scaled to isotopes, which have not yet been measured.

<sup>\*</sup> Contribution to the Topical Issue “Perspectives on Nuclear Data for the Next Decade” edited by Nicolas Alamanos, Eric Bauge, Stéphane Hilaire.

<sup>a</sup> e-mail: Stephan.OBERSTEDT@ec.europa.eu

In the following we attempt to summarize and to discuss achievements made in the past without the claim of being complete. However, the data collected during the past and, in particular, their selective entrance into evaluated nuclear data files and nuclear model calculations is the origin of the today's high priority requests on prompt fission  $\gamma$ -ray data [9, 10]. Next, we present recent measurement campaigns undertaken in response to the data requests published by the OECD Nuclear Energy Agency (NEA) [11]. We will end with an outlook on open questions and future data needs. Up-coming measurement campaigns and their associated instrument developments will be presented.

## 2 History of prompt fission $\gamma$ -ray measurements

The investigation of prompt fission  $\gamma$ -ray emission started in the 1950 years, amongst which the measurement of spectral data from the spontaneous fission of  $^{252}\text{Cf}$  using tellurium-doped sodium-iodine scintillation detectors, NaI(Tl) [12]. First correlated measurements of prompt fission  $\gamma$ -ray as a function of the fragment kinetic energy were made by Milton and Fraser [13], and spectra for different fragment mass ratios were published in 1964 [14], employing a germanium detector. In this experiment the Doppler-shift due to the emission from moving fragments were detected putting a limit on the  $\gamma$  emission time relative to the instance of fission.

In the 1970 years a systematic study of prompt fission  $\gamma$ -ray (PFG) emission was conducted. There are several studies on spontaneous fission of  $^{252}\text{Cf}$  [15] and thermal-neutron-induced fission on  $^{235}\text{U}$  [15–17],  $^{233}\text{U}$  [17, 18] and  $^{239}\text{Pu}$  [15, 18]. The energy range for  $\gamma$ -rays was extended down to 10 keV [16] and up to 8 MeV. All experiments were carefully designed to match the flight path length with the timing resolution of the NaI  $\gamma$ -ray detectors. Time dependence of PFG emission was investigated up to 275 ns after fission [18], showing that the distinction from the neutron-induced  $\gamma$ -ray component becomes increasingly difficult. *One* reason is the limited pulse-height resolution of sodium-iodine based scintillation detectors, which do not allow suppressing this component by pulse-height analysis.

The data from ref. [15] for  $^{252}\text{Cf}$ ,  $^{235}\text{U}$  and  $^{239}\text{Pu}$  was used for spectrum evaluation and adapted for neighboring isotopes. Due to the lack of experimental data no change of spectral shape as a function of excitation energy was considered.

Very early, attempts were made to determine prompt  $\gamma$ -ray lifetimes and isomer decay of fission fragments [19–24]. In 1971 Albinsson published decay curves and half-lives of  $\gamma$ -emitting states in thermal-neutron-induced fission on  $^{235}\text{U}$ . Half-lives down to 7.5 ps were measured using a collimator, which was moved along the fission axis [25]. It was concluded that about 70% of the prompt  $\gamma$ -rays is emitted within 60 ps. In another experiment, based on the velocity of the fragment and a variable distance between fission source and particle detector, life-

times in the range of 100 ps and 2 ns of non Doppler-shifted  $\gamma$ -lines could be determined [26]. In a similar experiment shadow cones were used in conjunction with high-resolution X-ray and  $\gamma$ -ray detectors, which allowed the identification of isotopes and associate  $\gamma$ -rays from (nearly) stopped fission fragments [27]. In total 130 transitions in the energy range from 0.01 to 1.5 MeV and emission times between 1 ns and 3  $\mu\text{s}$  were assigned to specific isotopes.

An interesting spectral measurement up to  $\gamma$ -ray energies of 19 MeV was conducted by Dietrich *et al.* in 1974 [28], which revealed a strong change of the spectral shape at  $E_\gamma \approx 8$  MeV. It took about 20 years before another measurement was conducted by van der Ploeg *et al.* [29, 30], which confirmed this observed spectral feature.

The angular distribution of prompt fission  $\gamma$ -rays relative to the fission axis started to be investigated in the mid 1960 years [31, 32]. Investigations were resumed in the 1970s which led to the confirmation of the previous results [33, 34]. As summarized in the review article from Nifenecker [35] the angular anisotropy amounts to about 15%. Investigations of the angular distribution relative to the fission axis of  $2^+ \rightarrow 4^+$  transitions in even-even nuclei ground state bands indicate that the initial fragment spin is oriented perpendicular. When looking on the integral prompt fission spectrum below 1.2 MeV the anisotropy still amounts to at least 13% [33, 36]. From that it appears that those  $\gamma$ -rays are essentially from quadrupole transitions ( $E2$ ) with a possible small admixture of dipole ( $E1$ ) radiation.

The  $\gamma$ -ray anisotropy as a function of fission-fragment properties was investigated in thermal-neutron-induced fission on  $^{235}\text{U}$  only. The anisotropy is constant for total kinetic energies (TKE) between 150 and 170 MeV and increases for higher TKE values. An increase of the anisotropy for TKE values smaller than 150 MeV cannot be excluded (cf. fig. 7 in ref. [35], p. 127). For average fragment mass-ratios between 1.2 and 1.8 the anisotropy does not change within the uncertainties, still the average anisotropy seems to be higher in heavier fragments with respect to the lighter partner.

Up to now, we only considered those experiments where essentially single detector measurements were conducted. Those allow for determining average spectral quantities, as, *e.g.*, the average  $\gamma$ -ray multiplicity and average total energy release per fission. Another type of detector, based on gadolinium-loaded liquid scintillators [37], has been employed providing information about the distribution of the total prompt  $\gamma$  energy per fission. Those instruments are generally used when measuring prompt neutron emission but the time structure of the registered events allows separating between neutrons and prompt  $\gamma$ -rays. Therefore, information also about the total  $\gamma$ -ray energy per fission is accessible [38, 39]. With the scintillator tank the dependence of prompt neutron and  $\gamma$ -ray emission on the excitation energy was investigated. In ref. [38] neutron multiplicity,  $\nu_p$  and average total  $\gamma$ -ray energy,  $\overline{E_\gamma}$  were investigated on  $^{235}\text{U}$  and  $^{239}\text{Pu}$  for the incident neutron energy region between 2 and 50 eV, *i.e.* where the fission cross-section shows a distinct resonance structure.

In the latter fissioning system an anti-correlation between  $\overline{E}_\gamma$  and  $\nu_p$  was observed for  $1^+$  resonances. This was interpreted as a signature of the  $(n, \gamma f)$  reaction, where a  $\gamma$ -ray is emitted prior to fission, leading to an increase of  $\overline{E}_\gamma$  and a decrease of  $\nu_p$ . No significant correlation was found for  $0^+$  resonances and in the resonance-neutron-induced fission on  $^{235}\text{U}$ . In ref. [39]  $\nu_p$  and the total  $\gamma$ -ray energy,  $E_\gamma$ , were measured on  $^{232}\text{Th}$ ,  $^{235}\text{U}$  and  $^{237}\text{Np}$  up to incident neutron energies of 15 MeV. A strong linear correlation between both average observables was found for all three fissioning compound nuclei. This correlation was already found in measurements of those quantities as a function of fission fragment mass in spontaneous fission of  $^{252}\text{Cf}$  (cf. ref. [35] and references therein). The deduction of the average  $\gamma$  multiplicity and the mean energy per photon was extracted by making an assumption about the multiplicity distribution and the shape of the  $\gamma$ -ray spectrum. Those assumptions of ref. [39] may be subject of discussions as the knowledge of these quantities improves.

The correlation between prompt neutron multiplicity and average total  $\gamma$ -ray energy was taken up by Valentine [40], who established systematic trends allowing to determine PFGS characteristics for different fissioning isotopes from measured prompt neutron multiplicities.

### 3 Renaissance of prompt fission $\gamma$ -ray measurements

With the development of advanced Generation-IV nuclear reactors, the need of new PFGS data became imminent. Since four out of six contemplated Generation-IV reactors require a fast neutron spectrum, a wider range of incident neutron energies has to be considered [9, 10]. Modeling of innovative core designs shows that, despite the numerous experiment campaigns reported in the previous section, the uncertainties on the existing PFG data are such that even in the standard thermal power reactors the  $\gamma$ -heating can locally be under-predicted by up to 30%, whereas an accuracy within 7.5% is requested. As a consequence an urgent data request was formulated for the relevant isotopes in the fuel of thermal power reactors,  $^{235}\text{U}$  and  $^{239}\text{Pu}$ , and included into the high-priority data request list (HPRL) of the OECD/NEA [11]. It requires an accuracy of 7.5% on the total prompt  $\gamma$ -heat production for the whole range of incident neutron energies relevant for thermal and fast power reactors.

As a consequence of recent instrumental advancements like the development of new  $\gamma$ -ray detectors [41, 42] as well as digital data acquisition systems, the determination of new and improved PFGS characteristics became possible with high precision. The recent installation of a kinematically focused neutron beam [43] enables the background-free investigation of prompt  $\gamma$ -ray emission in fast-neutron-induced fission on both fissile and non-fissile actinide isotopes.

### 4 Recent achievements

During the last five years we have measured PFGS characteristics for the spontaneous fission of  $^{252}\text{Cf}$  [44], thermal-

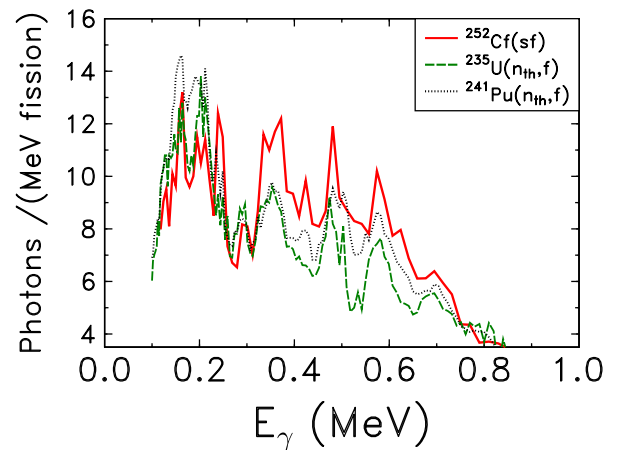


**Fig. 1.** (Color online) Prompt fission  $\gamma$ -ray spectra from  $^{252}\text{Cf}(\text{sf})$  [44],  $^{235}\text{U}(\text{n}_{\text{th}}, \text{f})$  [45] and  $^{241}\text{Pu}(\text{n}_{\text{th}}, \text{f})$  [46] with focus on the low-energy part of the spectrum showing a distinct structure (for details see text); all spectra were taken with cerium-doped lanthanum-bromide ( $\text{LaBr}_3:\text{Ce}$ ) detectors of size  $5.1 \text{ cm} \times 5.1 \text{ cm}$  (diameter  $\times$  length of the crystal).

neutron-induced fission on  $^{235}\text{U}$  [45] and  $^{241}\text{Pu}$  [46] as well as fast-neutron-induced fission of  $^{235,238}\text{U}$  [47, 48]. All experiments were performed with different cerium-doped lanthanum-bromide ( $\text{LaBr}_3:\text{Ce}$ ) and cerium-bromide detectors of size  $5.1 \text{ cm} \times 5.1 \text{ cm}$  (diameter  $\times$  length of the crystal). As fission triggers we used Frisch-grid ionization chambers [49, 50] and poly-crystalline diamond detectors [51]. The response of the  $\gamma$ -detectors was simulated with the Monte-Carlo code PENELOPE2011 [52]. From the emission spectra we determined average values for multiplicity and total energy per fission. As detailed in refs. [44–46] all detectors gave consistent results (within  $1\sigma$ ) with individual uncertainties on the PFGS characteristics smaller than 5%. In all cases the average total  $\gamma$ -ray energy per fission,  $\overline{E}_{\gamma, \text{tot}}$ , was determined with an accuracy better than 2% ( $1\sigma$ ). The quoted uncertainty comprises statistical ( $\approx 10\%$ ) and systematic ( $\approx 90\%$ ) uncertainties. Systematic uncertainties are from simulation of the detector response ( $\approx 55\%$ ), energy calibration ( $\approx 4\%$ ) and fitting the detector response ( $\approx 31\%$ ).

Prompt  $\gamma$ -rays were selected within a time-window of  $\pm 3 \text{ ns}$ . For all isotopes discussed up to here the average total prompt  $\gamma$ -ray energy turns out to be higher by a few percent compared to literature. The observed excess for  $^{235}\text{U}$  and  $^{241}\text{Pu}$  is 5.2% and 3.2%, respectively, relative to the values found in ENDF/B-VII.1 (see table 1).

Investigation of two adjacent time-bins, ranging from 4–7 and 8–10 ns, showed that contributions from isomeric decay may account for about 5% of the prompt photons. However, at this stage of our investigations, this might be regarded as an upper limit, because not all possible components from inelastic prompt neutron scattering, at neutron energies between 6.4 and 12 MeV, in the detector are definitely excluded yet in the last time bin.

The low-energy part of the emission spectra are depicted in fig. 1. A striking feature is the distinct structure

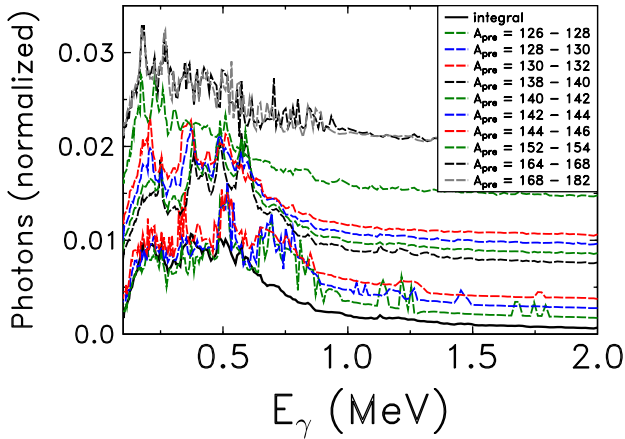


**Fig. 2.** (Color online) Prompt fission  $\gamma$ -ray spectra for  $^{252}\text{Cf}$  (sf) [53] as a function of fragment mass, for nominal mass bins of  $\Delta A = 2$ , with focus on energies below 2 MeV are shown and compared to the integral spectrum (black full line); each spectrum is normalized and offset for better visibility.

in the spectra of all isotopes, which may be observed at  $\gamma$ -ray energies below 0.8 MeV. In a first correlation experiment on spontaneous fission of  $^{252}\text{Cf}$ , using a twin Frisch-grid ionization chamber for fission-fragment detection, we started to look into correlations between the observed structure and fission-fragment characteristics, *e.g.* mass and kinetic energy. In fig. 2 prompt fission  $\gamma$ -ray spectra from the spontaneous fission of  $^{252}\text{Cf}$  as a function of the fragment mass, for nominal mass bins of  $\Delta A = 2$ , are shown with the focus on energies below 2 MeV; each spectrum is normalized and offset for better visibility. For further details on this experiment we refer to a forthcoming publication [53]. The strong spectral shape changes with the mass-cut are evident and open up the possibility to benchmark theoretical models on prompt  $\gamma$ -ray emission.

Albeit the energy resolution of lanthanide-halide detectors cannot compete with that of a high-purity germanium (HPGe) detector, the correlation of  $\gamma$ -emission and fragment properties may enable identification and spectroscopy of very neutron-rich isotopes, which can only be produced in nuclear fission. Tagging additionally on isomeric  $\gamma$ -decay in coincidence with prompt  $\gamma$ -rays will enhance the sensitivity of those investigations. First and promising results on this topic will be subject of a forthcoming publication.

With the directional fast-neutron beam LICORNE, which became recently operational at the Institut de Physique Nucléaire (IPN) in Orsay (France), we started first PFGS studies on  $^{235}\text{U}$  and  $^{238}\text{U}$ . At LICORNE neutrons are produced in inverse kinematics with 16.5 MeV  $^7\text{Li}$  impinging on a hydrogen-containing material [43] or on a  $\text{H}_2$ -gas cell, which is already being implemented. The generated forward-directed neutrons have an energy between 0.5 and 4 MeV with a spectral shape similar to that of a typical fast-reactor spectrum. Details on the experiment will be described elsewhere [48]. As an example for

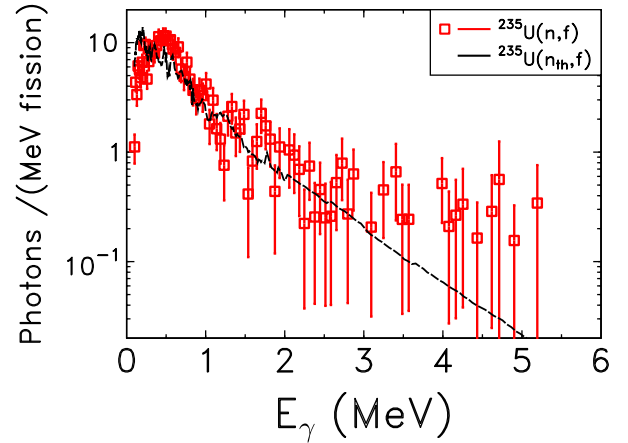


**Fig. 3.** (Color online) Prompt fission  $\gamma$ -ray spectrum (tentative) from the reaction  $^{235}\text{U}(n,f)$  at an average incident neutron energy of 1.5 MeV, taken with three  $\text{LaBr}_3:\text{Ce}$  detectors of size 5.1 cm  $\times$  5.1 cm (diameter  $\times$  length of the crystal) [48].

**Table 1.** Average total  $\gamma$ -ray energy per fission,  $\overline{E}_{\gamma,\text{tot}}$ , for the target isotopes discussed in this work [41,45,46,48]; our results are compared to the corresponding data from the ENDF/B-VII evaluated data file and ref. [55] together with the observed excess in % (right column). The value marked by (\*) is tentative. The value for  $\overline{E}_{\gamma,\text{tot}}$  indicated by (<sup>†</sup>) has been taken up in ref. [56] after the release of ENDF/B-VII.1 and is based on results from ref. [59] and disputed in ref. [57] (see text for more details).

Target isotope	$E_n$ (MeV)	Our work	Literature	Excess (%)
		$\overline{E}_{\gamma,\text{tot}}$ (MeV)	$\overline{E}_{\gamma,\text{tot}}$ (MeV)	
$^{252}\text{Cf}$	0	$6.63 \pm 0.08$	6.70 [7]	-1.1
$^{235}\text{U}$	thermal	$6.92 \pm 0.09$	6.58 [7]	5.2
	1.5	$7.4 \pm 0.7^{(*)}$	6.58 [7]	$12 \pm 2$
			$6.72 \pm 0.03$ [55]	$10 \pm 1$
$^{241}\text{Pu}$	thermal	$6.41 \pm 0.06$	6.19	3.6
			$7.52^{(\dagger)}$ [56]	-15

the new opportunities open to the nuclear community, a tentative emission spectrum from the reaction  $^{235}\text{U}(n,f)$  at an average incident neutron energy of 1.5 MeV, taken with three  $\text{LaBr}_3:\text{Ce}$  detectors similar to those described above, is shown in fig. 3 and compared with the spectrum obtained from thermal-neutron-induced fission. The attenuation visible at low  $\gamma$ -ray energies is corrected for when calculating the spectral characteristics as described in refs. [45,54]. As summarized in table 1, the average total  $\gamma$ -ray energy per fission,  $\overline{E}_{\gamma,\text{tot}}$  seems to increase with incident neutron energy. However, the presently still large uncertainty does not allow definitive conclusions yet.

Next we followed the above-mentioned idea of Valentine [40], who parametrized the PFGS characteristics as a function of average prompt neutron multiplicity, and determined new coefficients based on our new data. Whereas

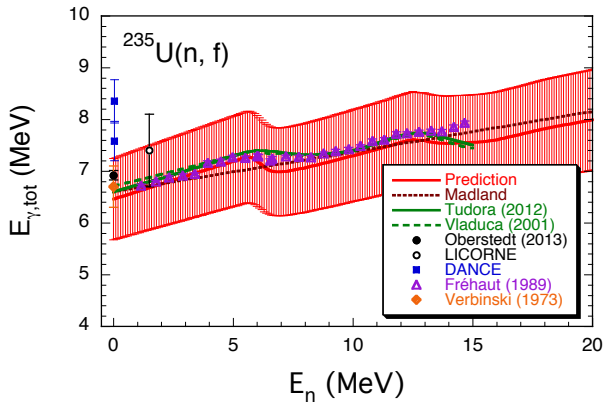


**Fig. 4.** (Color online) Average total  $\gamma$ -ray energy per fission,  $\overline{E}_{\gamma,\text{tot}}$  as a function of incident neutron energy,  $E_n$ , according to the recipe reported in ref. [57].

in ref. [40] only spontaneous and thermal-neutron-induced fission was taken into account we extended this concept to higher neutron energies [57]. As depicted in fig. 4, a general increase of  $\overline{E}_{\gamma,\text{tot}}$  as a function of incident neutron energy,  $E_n$ , is predicted with distinct slope changes at the thresholds for 2nd and 3rd chance fission. Our tentative experimental value for  $\overline{E}_{\gamma,\text{tot}}$  from the reaction  $^{235}\text{U}(n_{\text{th}}, f)$  is in reasonable agreement with the systematic trend.

The DANCE  $4\pi$   $\gamma$ -ray spectrometer [58] was recently also employed to measure PFGS data. The spectrometer is based on  $\text{BaF}_2$  detectors, which possess fast timing capabilities, but suffer from a much worse pulse-height resolution. The spectrometer allows measuring prompt  $\gamma$ -ray multiplicity distributions and to higher spectral energies. PFGS from the reactions  $^{235}\text{U}(n, f)$  and  $^{239,241}\text{Pu}(n, f)$  were measured, the results being summarized in ref. [59]. The spectra are integrated over an incident neutron energy range up to 100 keV. Details of the experiment are not subject to this paper. However, a general feature of the PFGS is the relatively high low-energy threshold and the negligence of inelastic (prompt fission) neutron scattering in the detector or surrounding structural material.

An interesting attempt was made to investigate the spectral shape as a function of incident neutron energy. With the FIGARO neutron detector array, based on liquid scintillation detectors [60], PFGS were measured for three different incident neutron energy bins, 1–2 MeV, 5–10 MeV and 10–20 MeV, *viz.* No spectral change was observed for  $\gamma$ -ray energies up to 4 MeV [61]. It is tempting to repeat those measurements with  $\gamma$ -ray detectors having a better pulse-height resolution.

## 5 The modeling of prompt fission $\gamma$ -ray emission

This paper puts a focus on experimental activities. Nevertheless, since there is an important mutual stimulation between theory or modeling and experiment, we would like to mention here briefly ongoing work on the modeling and theoretical description of prompt fission  $\gamma$ -ray emission.

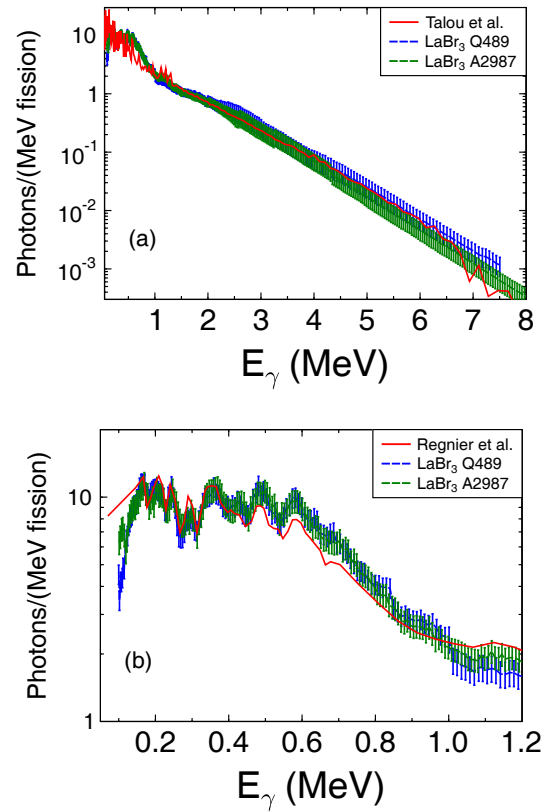


**Fig. 5.** (Color online) Prompt fission  $\gamma$ -ray spectra from the spontaneous fission of  $^{252}\text{Cf}$  for two  $\text{LaBr}_3\text{:Ce}$  detectors of different size [44, 54]; (a) Comparison of experimental data with calculations from ref. [62] and (b) with calculations from ref. [70] focussing on  $\gamma$ -ray energies below 1.2 MeV.

Without claiming of being complete we mention work recently performed at the Los Alamos National Laboratory (CGMF [62–65]), the Lawrence Livermore National Laboratory (FREYA [66–68]) and the CEA Cadarache (FIFRELIN [69–72]). Whereas FREYA uses analytical expressions based on Weisskopf’s statistical theory to describe neutron and  $\gamma$ -ray emission all other models are based essentially on the Monte Carlo Hauser-Feshbach statistical theory. In the latter type of models competition between neutron and  $\gamma$ -ray emission is incorporated as well.

In fig. 5 simulations of prompt fission  $\gamma$ -ray spectra from the spontaneous fission of  $^{252}\text{Cf}$  are shown. In the upper part a simulation performed with the CGMF code is shown, in the lower part the corresponding one obtained with FIFRELIN is shown for  $\gamma$ -ray energies below 1.2 MeV. In the latter case the competition between prompt neutron and prompt  $\gamma$ -ray emission is fully accounted for. In this way experimental data, especially when correlated with fission fragment mass and total kinetic energy, may help to reveal distinct ingredients for a proper description of the de-excitation of fission fragments, *e.g.* the functional dependence of the level density and the  $\gamma$  strength function.

Apart from the models mentioned above, two other approaches are proposed. The phenomenological point-by-point model [73, 74] is based on available experimental data and systematic behavior of model parameters. While so far no prompt fission  $\gamma$ -ray spectra have been published yet, at least some characteristic parameters are calculated for fast neutrons up to some tens of MeV. As an example some results are shown in fig. 4 for  $^{235}\text{U}(n, f)$  up to  $E_n = 15$  MeV. The GEF code is based on a semi-empirical model for a general description of the fission process, which covers most of the properties of fission fragments and the emitted neutrons and photons in a global and consistent way [75–77]. Its parameters are taken from existing experimental data, otherwise they are provided by a model calculation. Among all available output quantities,  $\gamma$ -ray spectra from prompt fission-induced by fast neutrons are given and their characteristics may be deduced. More detailed information about the underlying physics concepts of both approaches are found in the corresponding references.

## 6 Problem solved?

In table 1 we compare the average total  $\gamma$ -ray energy per fission,  $\overline{E}_{\gamma, \text{tot}}$ , for the target isotopes discussed with the corresponding values found in the ENDF/B-VII library. The most right column gives the relative excess energy in percent as obtained from the new PFGS data. For all thermal-neutron-induced reactions the new data shows a higher prompt  $\gamma$ -energy release of 3 to 8%. In case of  $^{235}\text{U}$ , one of the isotopes listed in the OECD/NEA HPRL, this excess is too small to fully account for the under-prediction of the prompt  $\gamma$ -heat. Since the evaluation for  $^{241}\text{Pu}$  is based on that of  $^{239}\text{Pu}$  we do not believe that the origin of the problem is caused from this isotope either<sup>1</sup>.

Although the heat excess measured for fast-neutron-induced fission is about two times higher than for thermal-neutron-induced fission one may not forget that the fission cross-section for fast neutrons is two orders of magnitude lower than for thermal neutrons. We suspect, therefore, that other sources in the prompt heat calculations contribute to the under-prediction.

As a first candidate we assume prompt  $\gamma$ -rays from the fast-neutron-induced fission on  $^{238}\text{U}$ . This data has hitherto not been measured and present evaluations could not be based on experimental data. However, the low fast-neutron-induced fission cross-section might compensate the 30 times higher abundance in the nuclear fuel.

Another source may be  $\gamma$ -induced fission from neutron-induced capture in the construction material around the nuclear fuel. Main constituents of the material are iron and nickel, which both release a considerable fraction of high-energy  $\gamma$ -rays after thermal neutron capture, *e.g.*  $E_\gamma \approx 9$  MeV from the reaction  $^{58}\text{Ni}(n_{th}, \gamma)$  contributes to about 50%. Of course, photo-fission cross-sections are relatively small reaching not far beyond 10 mb above  $E_\gamma > 7$  MeV,

<sup>1</sup> The second entry for  $^{241}\text{Pu}(n_{th}, f)$  was found in an apparent update of ENDF/B-VII [56]. The values are deduced from ref. [59] and disputed in ref. [57].

but the thermal-neutron capture rate on the construction material is immense inside and around the nuclear core, and this possible contribution is not yet considered in present reactor calculations [78].

Last, but definitely not least, possible isomeric decay has to be investigated more closely. Following consequently the definition of “prompt decay processes”, the integral time bin up to the onset of  $\beta$ -decay of fission fragments has to be fully accounted for. Based on the present knowledge about the decay properties of neutron-rich isotopes, decay times up to 1 ms might have to be considered. In order to do so, experimental setups have to be modified allowing a more efficient discrimination against ambient background radiation. The contribution of prompt fission neutrons, reaching the detector typically within the first micro-second after fission, must carefully be corrected for. Up to now this contribution has been fully suppressed by means of time-of-flight or corrected for within the first 10 ns as described above and in refs. [44–46].

## 7 Future $\gamma$ -ray data needs

Based on our evaluation of present day’s prompt fission  $\gamma$ -ray data, the problem of under-predicting the prompt heat production close to a reactor core is still persisting. In the following we attempt to formulate further data needs and to motivate a future measurement program. The strategy here should be twofold. First, future measurements should produce relevant nuclear data, which may eventually justify re-adjustments of evaluated nuclear data file entries. Second, experiments should aim at investigating more thoroughly correlations between prompt  $\gamma$ -ray and fission-fragment characteristics as well as with prompt neutron properties. Those measurements would help to understand how the excitation energy is shared between the two fission fragments and to improve modeling the de-excitation process in fission fragments, which is a necessary pre-requisite to benchmark nuclear theory and model calculations.

Based on the presently available measurement setup at the Joint Research Centre (JRC) IRMM, attempts should be made to enlarge the data base on PFGS characteristics from, *e.g.*, spontaneous fission of  $^{240,242}\text{Pu}$  and  $^{246,248}\text{Cm}$  as input for reducing the uncertainties on systematic trends as shown in fig. 4. Also measurements with thermal beams should be continued. Here, in first instance, prompt fission  $\gamma$ -ray emission in the thermal-neutron-induced fission on  $^{239}\text{Pu}$  will be measured in 2015 under the CHANDA Trans National Access scheme [79] in order to respond to the remaining entry H.4 on the OECD/NEA HPRL. For those measurements an efficient fission trigger like Frisch-grid ionization chambers [49, 50] or ultra-fast diamond detectors [51] should be employed.

At JRC-IRMM a new  $\gamma$ -ray spectrometer, called GLADIS (Geel Lathanide halide Detector array for Isomer Studies), was put in operation (see fig. 6). It consists of 8  $\text{CeBr}_3$  detectors of size  $5.1 \text{ cm} \times 5.1 \text{ cm}$  (diameter  $\times$  length of the crystal) and 4 high-purity coaxial germanium (HPGe) detectors with 45% relative efficiency. Ini-



**Fig. 6.** (Color online) Photograph of GLADIS, the new Geel Lathanide halide Detector array for Isomer Studies presently consisting of 4 HPGe detectors (45% rel. eff.) and 8 cerium-bromide detectors of size  $5.1\text{ cm} \times 5.1\text{ cm}$  (diameter  $\times$  length), taken during commissioning at a neutron flight-path station at JRC-IRMM.

tially designed for the investigation of shape-isomer population through resonance-neutron capture, it may serve also for a future PFGS measurement program. In a second phase GLADIS will be extended to 15 cerium-bromide detectors and up to 8 HPGe detectors.

Measurements on fast-neutron-induced fission on  $^{235}\text{U}$  and  $^{239}\text{Pu}$  are part of the high-priority data request from the OECD/NEA and are possible at the novel LICORNE forward-directed neutron beam. Using  $^7\text{Li}$  and  $^{11}\text{B}$  beams on a hydrogen target allows investigating PFGS characteristics up to an incident neutron energy  $E_n = 12\text{ MeV}$ . When, in the near future, the NFS (Neutrons for Science) [80] facility will be operational, a second neutron beam will be available to the community extending the energy range to  $E_n = 40\text{ MeV}$ . Those data will serve as benchmark for present and future systematics.

At LICORNE PFGS characteristics of non-fissile isotopes relevant for the nuclear fuel cycle can be investigated. Here, of course, emphasis has to be put on the development of compact (multi-layer) fission detectors to provide a sufficiently high fission rate and to employ large-area  $\gamma$ -spectrometers, preferential made of lanthanide-halide (*e.g.*, GLADIS, PARIS [81]) or  $\text{BaF}_2$  detectors. While the first detector type provides good energy resolution and fast timing capabilities the latter are available at much larger sizes and, thus higher efficiency, at comparable timing characteristics but much worse energy resolution.

Investigations of photon-induced reactions will serve twofold. Firstly, PFGS data from photo-fission of  $^{232}\text{Th}$ ,  $^{234,235,238}\text{U}$  and  $^{239-242}\text{Pu}$  serve as input to establish and test systematic trends and for benchmarking de-excitation models. Those targets can be made available; some of them of spectroscopic quality, to, secondly, allow investigating correlations with fission fragment characteristics. With the S-DALINAC bremsstrahlung facility [82] at the Darmstadt Technical University or the future ELI-NP [83–85] high-intense mono-energetic photon source at

IFINN, Bucharest, excellent facilities for this part of the measurement program are or will soon be available.

In order to accomplish a full understanding of the de-excitation mechanism in nuclear fission, prompt neutron- $\gamma$ -fission fragment correlations should be investigated as well. At the JRC-IRMM an array of 13 neutron detectors, called SCINTIA, was recently made operational. It will be extended with lanthanide-halide detectors. For this an ionization chamber with  $\cos\theta$ - and  $\phi$ -resolution was developed. In a first experiment prompt fission neutron and  $\gamma$ -ray spectra from resonance-neutron-induced fission on  $^{235}\text{U}$  are being measured. Possible contribution from  $(n, \gamma f)$  will be investigated.

Finally, it is worthwhile to underline that a large fraction of the contemplated measurement program requires considerable beam time at accelerator-driven neutron sources or research reactors together with the associated man power for performing the experiments and the subsequent data analysis. Therefore, we recommend that at least parts of the proposed measurement program will be taken up as high priority nuclear data requests by the OECD/NEA in order to stimulate sufficient support.

One of the authors (RB) is indebted to the European Commission for providing a PhD fellowship at EC JRC-IRMM, during which part of this work was carried out. This work was also supported by the European Commission in the framework of the EFNUDAT program (Agreement No. 31027) as well as the ERINDA program (Agreement No. 269499), which is hereby gratefully acknowledged.

**Open Access** This is an open access article distributed under the terms of the Creative Commons Attribution License (<http://creativecommons.org/licenses/by/4.0>), which permits unrestricted use, distribution, and reproduction in any medium, provided the original work is properly cited.

## References

1. J.C. Browne, F.S. Dietrich, *Phys. Rev. C* **10**, 2545 (1974).
2. G.S. Boikov, V.D. Dmitriev, G.A. Kudyaev, Yu.B. Ostapenko, M.I. Svirin, G.N. Smirenkin, *Sov. J. Nucl. Phys.* **53**, 392 (1991).
3. G.N. Lovchikova, A.M. Trufanov, M.I. Svirin, V.A. Vinogradov, A.V. Polyakov, *Phys. At. Nucl.* **67**, 1246 (2004).
4. S. Lemaire, P. Talou, T. Kawano, M.B. Chadwick, D.G. Madland, *Phys. Rev. C* **72**, 024601 (2005).
5. N. Kornilov, F.-J. Hamsch, I. Fabry, S. Oberstedt, T. Belgya, Z. Kis, L. Szentmiklosi, S. Simakov, *Nucl. Sci. Eng.* **165**, 117 (2010).
6. A. Tudora, F.-J. Hamsch, S. Oberstedt, *Nucl. Phys. A* **917**, 43 (2013).
7. ENDF/B-VII Evaluated Nuclear Data File, <http://www.nndc.bnl.gov/exfor/endl00.jsp>.
8. JEFF 3.1 Joint European Fusion File, [https://www.oecd-neo.org/dbdata/nds\\_jefreports/jefreport-22/nea6807-jeff22.pdf](https://www.oecd-neo.org/dbdata/nds_jefreports/jefreport-22/nea6807-jeff22.pdf).
9. G. Rimpault, A. Courcelle, D. Blanchet, Comment to the HPRC: ID H.3 and H.4.

10. G. Rimpault, in *Proceedings of the Workshop on Nuclear Data Needs for Generation IV, April 2005*, edited by P. Rullhusen (World Scientific, Singapore, 2006) p. 46.
11. Nuclear Data High Priority Request List of the NEA (Req. ID: H.3, H.4), <http://www.nea.fr/html/dbdata/hprl/hprlview.pl?ID=421> and <http://www.nea.fr/html/dbdata/hprl/hprlview.pl?ID=422>.
12. A.B. Smith, P.R. Fields, A.M. Friedman, *Phys. Rev.* **104**, 669 (1956).
13. J.C.D. Milton, J.S. Fraser, *Phys. Rev.* **111**, 877 (1958).
14. H.R. Bowman, S.G. Thompson, J.O. Rasmussen, *Phys. Rev. Lett.* **12**, 195 (1964).
15. V.V. Verbinski, H. Weber, R.E. Sund, *Phys. Rev. C* **7**, 1173 (1973).
16. R.W. Peelle, F.C. Maienschein, *Phys. Rev. C* **3**, 373 (1971).
17. F. Pleasonton, R.L. Ferguson, H.W. Schmitt, *Phys. Rev. C* **6**, 1023 (1972).
18. F. Pleasonton, R.L. Ferguson, H.W. Schmitt, *Phys. Rev. A* **213**, 413 (1973).
19. H. Maier-Leibnitz, P. Armbruster, H.J. Specht, *Phys. and Chem. of Fission 1965*, Vol. **II**, *Proc. of a Symp., Salzburg, 22-26 March 1965*, IAEA, Vienna, STI/PUB/101 (1965) 113.
20. F.C. Maienschein, R.W. Peele, W. Zobel, T.A. Love, *2nd U.N. Int. Conf. on Peaceful Uses of Atomic Energy, Geneva 1958*, Vol. **15** (U.N. Geneva, 1958) 366.
21. S.A.E. Johansson, *Nucl. Phys.* **60**, 378 (1964).
22. P. Armbruster, F. Hossfeld, H. Labus, K. Reichelt, *Phys. and Chem. of Fission 1973*, Vol. **II**, *Proc. of a Symp., Vienna, 28 July-1 August 1969*, IAEA, Vienna, STI/PUB/234 (1969) 545.
23. G.V. Val'skii, D.M. Kaminker, G.A. Petrov, L.A. Popeko, *Sov. At. Energy* **18**, 279 (1965).
24. J. Higbie, AE-374, AB Atomenergi (1969).
25. H. Albinsson, *Phys. Scr.* **3**, 113 (1971).
26. R.C. Jared, H. Nifenecker, S.G. Thompson, *Phys. and Chem. of Fission 1973*, Vol. **II**, *Proc. of a Symp., Rochester, New York, 13-17 August 1973*, IAEA, Vienna, STI/PUB/347 (1974) 211.
27. R.G. Clark, L.E. Glendenin, W.L. Talbert Jr., *Phys. and Chem. of Fission 1973*, Vol. **II**, *Proc. of a Symp., Rochester, New York, 13-17 August 1973*, IAEA, Vienna, STI/PUB/347 (1974) 221.
28. F.S. Dietrich, J.C. Browne, W.J. O'Connell, M.J. Kay, *Phys. Rev. C* **10**, 795 (1974).
29. H. van der Ploeg, C.R. Laurens, J.C.S. Bacelar, T. van der Berg, V.E. Iacob, J.R. Jongman, A. van der Woude, *Phys. Rev. Lett.* **68**, 3145 (1992) **69**, 1148(E) (1992).
30. H. van der Ploeg, J.C.S. Bacelar, A. Buda, C.R. Laurens, A. van der Woude, *Phys. Rev. C* **52**, 1915 (1995).
31. M.M. Hoffman, *Phys. Rev. B* **133**, 714 (1964).
32. O.I. Ivanov, Y.A. Kushner, G.N. Smirenkin, *Zh. Ehksp. Teo. Fiz. Pis'ma* **6**, 898 (1967).
33. P. Armbruster, H. Labus, K. Reichelt, *Z. Naturforsch. A* **26**, 512 (1971).
34. J.B. Wilhelmy, E. Cheifetz, R.C. Jared, S.G. Thompson, H.R. Bowman, J.O. Rasmusson, *Phys. Rev. C* **5**, 2041 (1972).
35. H. Nifenecker, C. Signarbieux, R. Babinet, J. Poitou, *Phys. and Chem. of Fission 1973*, Vol. **II**, *Proc. of a Symp., Rochester, New York, 13-17 August 1973*, IAEA, Vienna, STI/PUB/347 (1974) 117.
36. K. Skarsvag, *Phys. Rev. C* **22**, 638 (1980).
37. J. Frehaut, *Nucl. Instrum. Methods* **135**, 511 (1976).
38. J. Frehaut, D. Shackleton, *Phys. and Chem. of Fission 1973*, Vol. **II**, *Proc. of a Symp., Rochester, New York, 13-17 August 1973*, IAEA, Vienna, STI/PUB/347 (1974) 201.
39. J. Frehaut, INDC(NDS)-220 (1989) 99.
40. T.E. Valentine, *Ann. Nucl. Energy* **28**, 191 (2001).
41. R. Billnert, S. Oberstedt, E. Andreotti, M. Hult, G. Marisens, A. Oberstedt, *Nucl. Instrum. Methods A* **647**, 94 (2011).
42. A. Oberstedt, S. Oberstedt, R. Billnert, W. Geerts, F.-J. Hamsch, J. Karlsson, *Nucl. Instrum. Methods A* **668**, 14 (2012).
43. M. Lebois, J.N. Wilson, P. Halipré, B. Leniau, I. Matea, A. Oberstedt, S. Oberstedt, D. Verney, *Nucl. Instrum. Methods A* **735**, 145 (2014).
44. R. Billnert, F.-J. Hamsch, A. Oberstedt, S. Oberstedt, *Phys. Rev. C* **87**, 024601 (2013).
45. A. Oberstedt, T. Belgya, R. Billnert, R. Borcea, T. Bryś, W. Geerts, A. Göök, F.-J. Hamsch, Z. Kis, T. Martinez, S. Oberstedt, L. Szentmiklosi, K. Takács, M. Vidali, *Phys. Rev. C* **87**, 051602 (2013).
46. S. Oberstedt, R. Billnert, T. Belgya, T. Bryś, W. Geerts, C. Guerrero, F.-J. Hamsch, Z. Kis, A. Moens, A. Oberstedt, G. Sibbens, L. Szentmiklosi, D. Vanleeuw, M. Vidali, *Phys. Rev. C* **90**, 024618 (2014).
47. M. Lebois, J.N. Wilson, P. Halipré, B. Leniau, I. Matea, A. Oberstedt, S. Oberstedt, D. Verney, *Phys. Proc.* **59**, 37 (2014).
48. M. Lebois, J.N. Wilson, P. Halipré, B. Leniau, I. Matea, A. Oberstedt, S. Oberstedt, D. Verney, to be submitted.
49. A. Göök, F.-J. Hamsch, A. Oberstedt, S. Oberstedt, *Nucl. Instrum. Methods A* **664**, 289 (2012).
50. A. Al-Adili, F.-J. Hamsch, R. Bencardino, S. Pomp, S. Oberstedt, Sh. Zeynalov, *Nucl. Instrum. Methods A* **671**, 103 (2012).
51. S. Oberstedt, R. Borcea, T. Bryś, Th. Gamboni, W. Geerts, F.-J. Hamsch, A. Oberstedt, M. Vidali, *Nucl. Instrum. Methods A* **714**, 31 (2013).
52. <http://www.oecd-nea.org/tools/abstract/detail/nea-1525>.
53. S. Oberstedt, A. Oberstedt, R. Billnert, to be submitted.
54. A. Oberstedt, R. Billnert, F.-J. Hamsch, S. Oberstedt, *Phys. Rev. C*, in press.
55. D.G. Madland, *Nucl. Phys. A* **722**, 113 (2006).
56. ENDF/B-VII Evaluated Nuclear Data File, <http://www.nndc.bnl.gov/exfor/endl00.jsp> (viewed on 2015-06-10).
57. A. Oberstedt, R. Billnert, S. Oberstedt, to be submitted.
58. M. Heil, R. Reifarth, M.M. Fowler, R.C. Haight, F. Käppeler, R.S. Rundberg, E.H. Seabury, J.L. Ullmann, J.B. Wilhelmy, K. Wisshak, *Nucl. Instrum. Methods A* **459**, 229 (2001).
59. A. Chyzh, C.Y. Wu, E. Kwan, R.A. Henderson, J.M. Gostic, T.A. Bredeweg, A. Couture, R.C. Haight, A.C. Hayes-Sterbenz, M. Jandel, H.Y. Lee, J.M. O'Donnell, J.L. Ullmann, *Phys. Rev. C* **87**, 034620 (2013).
60. R.C. Haight, J.M. O'Donnell, L. Zanini, M. Devlin, D. Rochman, in: J. Kvasil, P. Cejnar, M. Krťicka (Editors), *Proc. Capture Gamma-Ray Spectroscopy and Related Topics, Pruhonice, Prague, Czech Republic, September 2-6, 2002*, Charles University, Prague, Czech Republic (World Scientific Publishing Co., 2003) 451.



61. E. Kwan, C.Y. Wu, R.C. Haight, H.Y. Lee, T.A. Bredeweg, A. Chyzh, M. Delvin, N. Fotiades, J.M. Gostic, R.A. Henderson, M. Jandel, A. Laptev, R.O. Nelson, J.M. O'Donnell, B.A. Perdue, T.N. Teddeucci, J.L. Ullmann, S.A. Wender, Nucl. Instrum. Methods A **688**, 55 (2012).
62. B. Becker, P. Talou, T. Kawano, Y. Danon, I. Stetcu, Phys. Rev. C **87**, 014617 (2013).
63. P. Talou, I. Stetcu, T. Kawano, Phys. Proc. **59**, 83 (2014).
64. P. Talou, T. Kawano, I. Stetcu, R. Vogt, J. Randrup, Nucl. Data Sheets **118**, 227 (2014).
65. I. Stetcu, P. Talou, T. Kawano, M. Jandel, Phys. Rev. C **90**, 024617 (2014).
66. R. Vogt, J. Randrup, Phys. Proc. **47**, 3 (2013).
67. R. Vogt, J. Randrup, Nucl. Data Sheets **118**, 220 (2014).
68. J.M. Verbeke, J. Randrup, R. Vogt, Comput. Phys. Commun. **191**, 178 (2015).
69. D. Regnier, O. Litaize, O. Serot, Phys. Proc. **59**, 59 (2012).
70. D. Regnier, Phys. Proc. **47**, 47 (2013).
71. O. Litaize, D. Regnier, O. Serot, Phys. Proc. **59**, 89 (2014).
72. O. Serot, O. Litaize, D. Regnier, Phys. Proc. **59**, 132 (2014).
73. A. Tudora, F.-J. Hamsch, S. Oberstedt, C. Manaiescu, Phys. Proc. **31**, 43 (2012).
74. A. Tudora, F.-J. Hamsch, S. Oberstedt, G. Giubega, I. Visan, Phys. Proc. **59**, 95 (2014).
75. K.-H. Schmidt, OECD/NEA, JEF/DOC 1398 (2012).
76. K.-H. Schmidt, B. Jurado, OECD/NEA, JEF/DOC 1423 (2012).
77. K.-H. Schmidt, B. Jurado, Ch. Amouroux, JEFF-Report 24, Data Bank, Nuclear-Energy Agency, OECD (2015).
78. I. Fabry, Nucl. Eng. Int., May 2014 edition and I. Fabry, private communication (2014).
79. <http://www.chanda-nd.eu>, and <http://win.ciemat.es/chanda/>.
80. X. Ledoux, M. Aïche, M. Avrigeanu, V. Avrigeanu, L. Audouin *et al.*, Nucl. Data Sheets **119**, 353 (2014).
81. <http://paris.ijf.edu.pl/>.
82. A. Göök, M. Chernykh, C. Eckardt, J. Enders, P. von Neumann-Cosel, A. Oberstedt, S. Oberstedt, A. Richter, Nucl. Phys. **851**, 1 (2011).
83. The ELI - Nuclear Physics Facility, [www.eli-np.ro](http://www.eli-np.ro).
84. D.L. Balabanski, the ELI-NP Science Team, Pramana **83**, 713 (2014).
85. P.G. Thirolf, L. Csige, D. Habs, M. Gunther, M. Jentschel, A. Krasznahorkay, D. Filipescu, T. Glodariu, L. Stroh, O. Tesileanu, H. Karwowski, G. Rich, EPJ Web of Conferences **38**, 08001 (2012).